

Numerical Study of Few-Cycle Pulses by Nonlinear Compression in Two-Photon Semiconductor Amplifiers

Noam Kaminski, Alex Hayat, Pavel Ginzburg, and Meir Orenstein

Abstract—Optical pulse compression down to a few optical cycles by the ultrabroadband gain of nonlinear two-photon process in semiconductors is proposed. Recent experimental demonstration of semiconductor two-photon gain (TPG) has motivated this analysis of ultrashort pulse dynamics with realistic semiconductor parameters. Comprehensive material model, including TPG, carrier depletion, linear absorption, Kerr effect, plasma response of injected carriers, and the material dispersion were numerically simulated using the finite-difference time-domain method. Pulse compression down to a few optical cycles is theoretically predicted.

Index Terms—Amplifiers, dispersive media, nonlinear optics, numerical analysis, semiconductor device modeling.

A considerable effort has been made to shorten optical pulsewidth from nanoseconds down to attoseconds [1]. Ultrashort pulses play a key role in various studies [2]–[4]. Robust pulsed lasers with pulses much shorter than 100 fs are highly required. Widely used techniques to generate short light pulses are based on mode-locked lasers [5], higher harmonic generation [1], [6], and nonlinearity in optical fibers [7]. However, these methods require highly complicated setups and cannot be implemented on a chip.

Here we present and provide a detailed study of an efficient pulse compression scheme, taking place within a simple and compact semiconductor device for compressing pulses from hundreds down to a few femtoseconds. The compression is achieved by propagating a pulse within a unique nonlinear semiconductor optical amplifier (SOA) exhibiting two-photon gain (TPG), based on the experiment in [8].

Theoretical prediction of what was considered at that time a very short pulse generation (~ 300 fs) in two-photon laser was reported in 1993 [9]. This analysis employed the nonlinear Schrödinger equation under the slowly varying envelope approximation (SVEA) for the electromagnetic fields, which holds for relatively wide pulses (much wider than the optical cycle). Moreover, in this TPG laser cavity, the gain saturation was assumed to be uniform over the whole pulse.

We theoretically predict and analyze a more complex situation: a compression of ultrashort pulses, beyond the electromagnetic SVEA, down to the limit of few cycle pulses in a

TPG semiconductor amplifier. For such ultrashort pulse propagation, uniform gain saturation assumption is not valid, and the actual dynamics of the saturation along the pulse must be considered. When such temporal effects are important, the split-step method as employed in [9] cannot be used and the finite-difference time-domain method is employed instead.

In a two-photon emission (TPE) process, electron transition between energy levels occurs by a generation of a photon pair. The rate of the stimulated TPE (W_{stim}) depends on the product of both photon densities n_1, n_2 and the electron transition matrix element W_0 [10]: $W_{\text{stim}} = (n_1 + 1)(n_2 + 1)W_0 \approx n_1 n_2 W_0$. An incident pair of photons will result in doubly stimulated TPE (TPG) only if their energies sum up to the electron-hole pair energy in the pumped material.

The nonlinear gain in TPG media is well-approximated by zero response time nonlinear equation, similar to other fast nonlinear optical processes [11]–[14]: $G(t) = g_0 E^2(t)$, where $E(t)$ is the pulse electric field envelope and g_0 is determined by the two-photon transition matrix element [8].

The nonlinear TPG is a favorable mechanism for pulse compression: strong fields at the pulse peak experience high gain, while weak fields at the pulse wings experience low gain, yielding a temporal width reduction. The significant advantage of semiconductor TPG over other compression methods is the combination of a strong nonlinearity and a wide spectral response [8]. The TPG bandwidth spans over the entire bandgap with additional broadening due to the carrier energy-distribution.

We consider an electrically pumped TPG semiconductor optical amplifying medium based on bulk GaAs. The resonant transition wavelength of GaAs is ~ 870 nm—slightly longer than half of the initial pulse carrier wavelength (telecommunication wavelength of $1.55 \mu\text{m}$). Under these conditions, the main interaction mechanism between the pulse and the gain medium is due to the TPG. We calculated the pulse propagation within the SOA including the following effects: TPG, carrier depletion induced saturation, linear loss, Kerr effect, complex plasma response of injected carriers, and full linear material dispersion of the SOA (see the Appendix for the parameters used).

The input is a 130-fs Gaussian pulse with peak intensity of 4.5 GW/cm^2 which corresponds to a typical experiment when an attenuated light from optical parametric oscillator is coupled into a semiconductor waveguide with $10 \mu\text{m} \times 10 \mu\text{m}$ crossection. This level is several orders of magnitude below the critical material damage threshold [13]. The input electric field must be strong enough so that the compression rate due to the TPG will be higher than the broadening rate due to the dispersion, while on the other hand too strong input will result in significant

Manuscript received July 27, 2008; revised November 03, 2008. First published December 09, 2008; current version published January 16, 2009.

The authors are with the Electrical Engineering Department, Technion, Haifa 32000, Israel (e-mail: mkaminsk@tx.technion.ac.il).

Color versions of one or more of the figures in this letter are available online at <http://ieeexplore.ieee.org>.

Digital Object Identifier 10.1109/LPT.2008.2009469

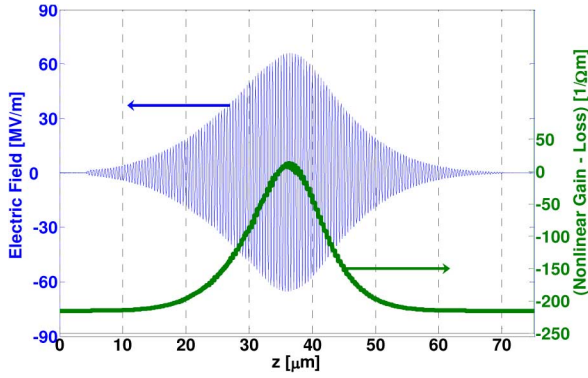


Fig. 1. Pulse electric field (blue) and net gain (green) versus the propagation distance at the first tens of micrometers of the SOA.

gain saturation and ceasing of compression. Thus, keeping the peak power relatively constant is a key consideration. Fig. 1 depicts the initial electric field (blue line) of the propagating pulse within the SOA. The gain is maximal around the pulse peak; in our case, net gain (nonlinear gain minus the loss) exists only between $z = 34.5 \mu\text{m}$ and $z = 38 \mu\text{m}$. The wings of the pulse have low field intensity and hence experience net loss.

Some parameters had only little influence on the pulse propagation. The negligible effect of the plasma resonance dependence on electron density is due to its resonance location around 60 meV, which is far from the pulse spectrum. Various additional nonlinear effects which can in principle accompany ultrafast pulse propagation appear to be nonsignificant. The refractive index change due to the nonlinear Kerr effect is, for the worst case, at the peak intensity of the final few cycles pulse, $\sim 0.3\%$. Thus the Kerr nonlinearity has almost no effect on the compression process where the intensity is much smaller and the propagation length is relatively short and when compared to the much stronger spectral broadening due to the gain nonlinearity. This was confirmed by our simulations which incorporated the Kerr nonlinearity. Stimulated Brillouin scattering threshold here is about 10^{22} W/m^2 —many orders of magnitude above the intensity considered. Stimulated Raman scattering (SRS) shift in GaAs is $\sim 30 \text{ meV}$ [15]. In order to distort the pulse, signal and pump wavelengths of SRS must be separated by less than the pulse bandwidth. In our simulations, this occurs only in the last few tens of micrometers causing a small spectral shift of a few meV. Second-harmonic generation (SHG) followed by one-photon gain may deplete the injected carrier density for very high intensities. Since there is no phase matching for the SHG, the generated photons have random momentum, and only a small fraction of them ($\beta = 10^{-4} - 10^{-5}$) are coupled to the waveguide. Our simulation shows that the power in the second-harmonic frequencies is less than 1% of the pulse power.

The saturated gain is modeled (neglecting polarization evolution effects) as

$$g(z, t) = \beta_0 \left(\frac{n(z, t)}{n_{\text{injec}}} \right) I(z, t)$$

$$\frac{\partial n(z, t)}{\partial t} = -g(z, t) \left(\frac{I(z, t)}{E_{\text{gap}}} \right) \quad (1)$$

where $g(z, t)$ is the nonlinear gain at position z and time t , $n(z, t)$ is the carrier density above transparency level, $n_{\text{injec}} =$

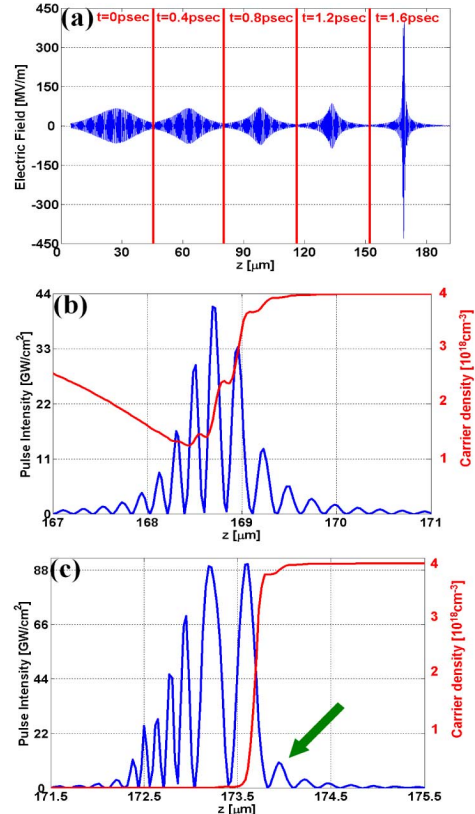


Fig. 2. (a) Five snapshots of the pulse electric field (blue) as function of location. Each snapshot is separated by a red thick line. (b) Snapshot of the pulse power (blue) and the carrier population inversion density (red) at $t = 1.6 \text{ ps}$. (c) The same as (b) only at $t = 1.65 \text{ ps}$.

$4 \times 10^{18} \text{ cm}^{-3}$ is the injected carrier density above transparency in steady state with no optical pulse present, $E_{\text{gap}} = 1.42 \text{ eV}$ is the GaAs bandgap, $I(z, t)$ is the pulse intensity, and $\beta_0 = 28 \text{ cm/GW}$ is the TPG coefficient calculated based on n_{injec} 10 times higher than in [14]—feasible in practical devices. The simplest two-level model predicts an increase of β_0 proportional to $n(z, t)$, and in semiconductors the gain increase is even stronger due to two-photon transition matrix element k -dependence [8]. Equation (1) was derived under two very plausible assumptions: the gain relaxation time (\sim picosecond) is much longer than the pulsewidth, preventing carrier population restoration during the femtosecond pulse; carrier diffusion during the femtosecond pulse can be neglected to—restricting the dynamics to local nonlinearity.

The pulse reshaping process is depicted in Fig. 2. Fig. 2(a) shows snapshots of the electric field as a function of location along the amplifier. The plot denoted by $t = 0 \text{ ps}$ represents the pulse immediately after entering the SOA, and the consecutive plots are the pulse at 400-fs intervals. In this example, the peak gain at $t = 0 \text{ ps}$ (Fig. 1) is very small while the loss at the wings is significantly larger, resulting in a slow increase of the peak power and a rapid decrease of the wings power. This process is illustrated in Fig. 2(a), showing a significant compression with almost no change in peak power till time $t = 1.2 \text{ ps}$.

At about $t = 1.2 \text{ ps}$, the pulse peak power reaches a critical value where the nonlinear gain is large enough to initiate a rapid growth of the peak power with simultaneous enhancement of the compression rate. The outcome of this compression is seen

at $t = 1.6$ ps. Fig. 2(b) shows the pulse power at time $t = 1.6$ ps where the pulsewidth is close to two half-cycles in power and the peak power is high enough to cause significant carrier depletion over less than half an optical cycle. Fig. 2(c) shows the pulse power 50 fs later. The carrier density is fully depleted by the leading edge of the first half-cycle, so that it is the only part of the pulse which is amplified, while the rest of the pulse, where $n_{(z,t)} = 0$, is in the transparency region. This is a cause for the apparent broadening (red shift) of the two major half-cycles [Fig. 2(b) and (c)].

At this stage, the full carrier depletion brings the compression process to a halt and the pulse envelope starts to rebroaden due to two main reasons: the dispersion, which becomes more significant as the pulsewidth is reduced; the dispersion length is only $38 \mu\text{m}$ for a 7.5-fs pulsewidth [16]. The second and more important effect is the depletion of the carrier density by the leading edge of the pulse before the arrival of the pulse peak. As a result, the leading edge of the pulse [marked in green arrow in Fig. 2(c)] grows while the rest of the pulse retains its amplitude. These two processes appear to be responsible for rebroadening of the pulse, but only by one cycle after $\sim 30 \mu\text{m}$ of propagation in the SOA. With the parameters used, the pulse is compressed to few cycles after propagating $\sim 170 \mu\text{m}$ down the SOA and it remains a few-cycles wide for at least additional few tens of micrometers.

When a pulse is a single cycle wide, its duration approaches that of the electron dephasing time [17] and the coherent effects of the carriers start to be significant and should be analyzed by Maxwell–Bloch equations; however, in the several-cycle regime of our analysis, the rate equation of (1) is still a good approximation.

In conclusion, we have shown that TPG is a feasible mechanism for pulse compression and it can be performed within a very compact semiconductor device. A 130-fs wide pulse was shown numerically to be compressed to a few-cycle pulse upon propagation of order of $100 \mu\text{m}$ in a TPG medium. The TPG device does not require any complex setup such as those used in conventional nonlinear optics, and can be easily integrated into semiconductor-based photonic circuits. The few cycles pulse is stable for a reasonable distance (tens of micrometers) inside the SOA, making the realization of practical TPG–based compressors appealing.

APPENDIX

MATERIAL AND NUMERICAL PARAMETERS

Simulation parameters: spatial and temporal resolutions are 30 nm and 0.05 fs, respectively. The linear dispersion [16], [18]

$$\begin{aligned} \varepsilon(\omega, z, t) &= 11 + \sum_{m=0}^3 \frac{G_m}{(E_m - \omega - j\delta)} + \frac{n_{(z,t)} q^2 \varepsilon_0 \tau^2}{m_e (E_{\text{plasma}} - \omega - j\tau^{-1})} \quad (2) \end{aligned}$$

where q is the electron charge, $\delta = 1$ meV is the phonon resonance width, ε_0 is free space permittivity, E_m are the various optical resonances of the material with G_m -corresponding resonance strength coefficients and $m_e = 0.067$ of electron mass is

TABLE I
PARAMETERS USED IN THE CALCULATIONS

Parameter	Value	Parameter	Value
n_2 (Kerr)	-1.7×10^{-10} [esu] [19]	n_0 (at λ_0)	3.374 [16]
E_3	0.033 [eV] [16]	τ	85 [fs] [17]
E_0	1.428 [eV] [16]	G_0	0.12 [eV] [16]
E_1	3 [eV] [16]	G_1	0.2 [eV] [16]
E_2	5.1 [eV] [16]	G_2	2 [eV] [16]
E_{plasma}	59.63 [meV] [17]	G_3	0.11 [eV] [16]
		Loss	122.5 cm^{-1}

the effective electron mass of GaAs. More parameters are shown in Table I.

REFERENCES

- [1] P. Antoine, A. L’Huillier, and M. Lewenstein, “Attosecond pulse trains using high-order harmonics,” *Phys. Rev. Lett.*, vol. 77, pp. 1234–1237, 1996.
- [2] T. Kobayashi, K. Nishimura, and E. Tokunaga, “Real-time spectroscopy of pseudoisocyanine J-aggregates with sub-5 fs lasers,” *J. Molecular Structure*, vol. 735–736, pp. 179–187, 2005.
- [3] A. H. Zewail, “Laser femtochemistry,” *Science*, vol. 242, pp. 1645–1653, 1988.
- [4] M. Lindberg and S. W. Koch, “Theory of coherent transients in semiconductor pump-probe spectroscopy,” *J. Opt. Soc. Amer. B*, vol. 5, pp. 139–146, 1988.
- [5] V. Cauterets, D. J. Richardson, R. Paschotta, and D. C. Hanna, “Stretched pulse Yb3+ silica fiber laser,” *Opt. Lett.*, vol. 22, pp. 316–318, 1997.
- [6] K. T. Kim, K. S. Kang, M. N. Park, T. Imran, G. Umesh, and C. H. Nam, “Self-compression of attosecond high-order harmonic pulses,” *Phys. Rev. Lett.*, vol. 99, no. 223904, 2007.
- [7] G. Chang, T. B. Norris, and H. G. Winful, “Optimization of supercontinuum generation in photonic crystal fibers for pulse compression,” *Opt. Lett.*, vol. 28, pp. 546–548, 2003.
- [8] A. Hayat, P. Ginzburg, and M. Orenstein, “Observation of two-photon emission from semiconductors,” *Nature Photon.*, vol. 2, pp. 238–241, 2008.
- [9] D. R. Heatley, W. J. Firth, and C. N. Ironside, “Ultrashort-pulse generation using two-photon gain,” *Opt. Lett.*, vol. 18, pp. 628–630, 1993.
- [10] D. Marcuse, *Principles of Quantum Electronics*. New York: Academic, 1980.
- [11] P. N. Butcher and D. Cotter, *The Elements of Nonlinear Optics*. New York: Cambridge Univ. Press, 1991.
- [12] R. M. Joseph and A. Taflov, “FDTD Maxwell’s equations models for nonlinear electrodynamics and optics,” *IEEE Trans. Antennas Propag.*, vol. 45, no. 3, pp. 364–374, Mar. 1997.
- [13] L. Huang, J. P. Callan, E. N. Glezer, and E. Mazur, “GaAs under intense ultrafast excitation: Response of the dielectric function,” *Phys. Rev. Lett.*, vol. 80, pp. 185–188, 1998.
- [14] C. N. Ironside, “Two-photon gain semiconductor amplifier,” *IEEE J. Quantum Electron.*, vol. 28, no. 4, pp. 842–847, Apr. 1992.
- [15] H. Oda, K. Inoue, N. Ikeda, Y. Sugimoto, and K. Asakawa, “Observation of Raman scattering in GaAs photonic-crystal slab waveguides,” *Opt. Express*, vol. 14, pp. 6659–6667, 2006.
- [16] E. D. Palik, *Handbook of Optical Constants of Solids*. Orlando, FL: Academic, 1985, vol. 1.
- [17] D. C. Scott, R. Binder, and S. W. Koch, “Ultrafast dephasing through acoustic plasmon undamping in nonequilibrium electron-hole plasmas,” *Phys. Rev. Lett.*, vol. 69, pp. 347–350, 1992.
- [18] R. Huber *et al.*, “Femtosecond buildup of coulomb screening in photoexcited GaAs probed via ultrabroadband THz spectroscopy,” *J. Lumin.*, vol. 94–95, pp. 555–558, 2001.
- [19] M. Sheik-Bahae, D. J. Hagen, and E. W. Van Stryland, “Dispersion and band-gap scaling of the electronic Kerr effect in solids associated with two-photon absorption,” *Phys. Rev. Lett.*, vol. 65, pp. 96–99, 1990.